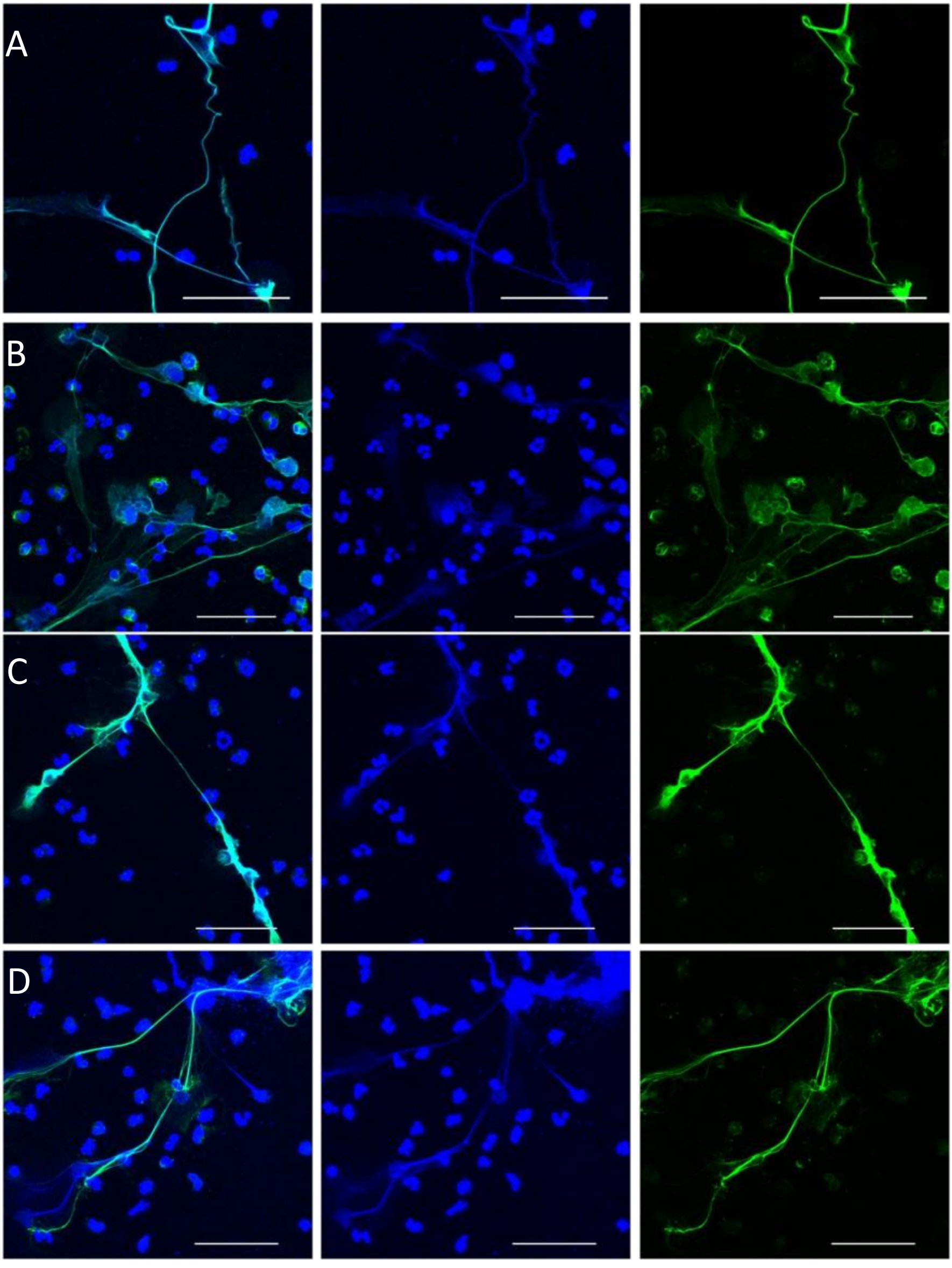


**Supplemental Figure 1. Identification of NETs in nonhuman primates.** In SIV-infected PTMs, filamentous structures released by neutrophils expressed Histone H3 (A); Myeloperoxidase (B); Lactoferrin (C); Elastase (D). NET biomarkers are all shown in green. Scale bar lengths: 50 µm. Nuclear staining: DAPI (blue).

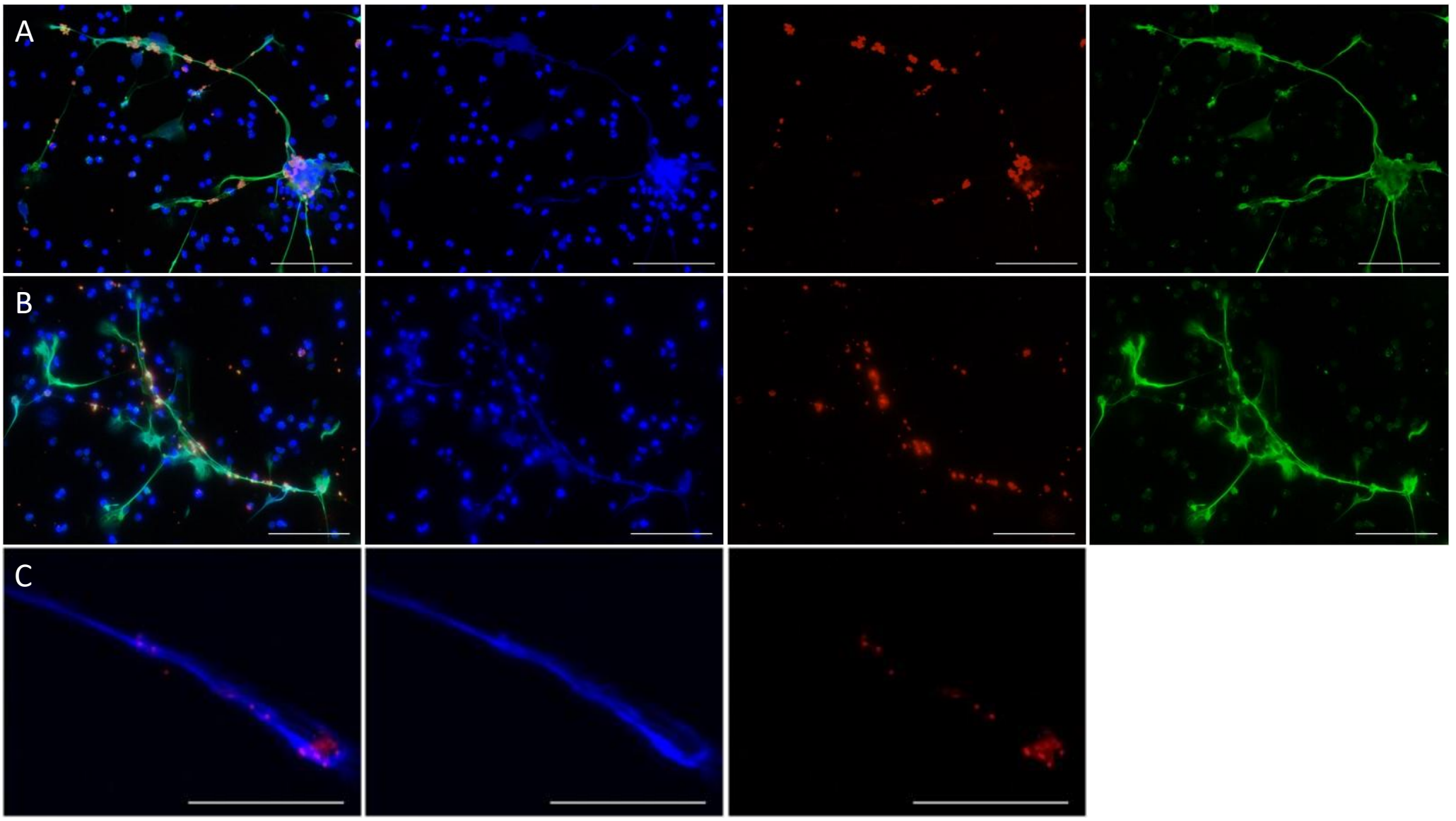


**Supplemental Figure 2**. **Microbes caught by NETs.** NETs generated by NHP neutrophils can capture bacteria such as (A) *Staphylococcus aureus* (red) and (B) *Escherichia coli* (red). NETs are also capable of capturing SIV virions (red) (C). NET identification: staining for lactoferrin (green). SIV detection: Scale bar lengths: 100 µm (A, B); 20 µm (C).

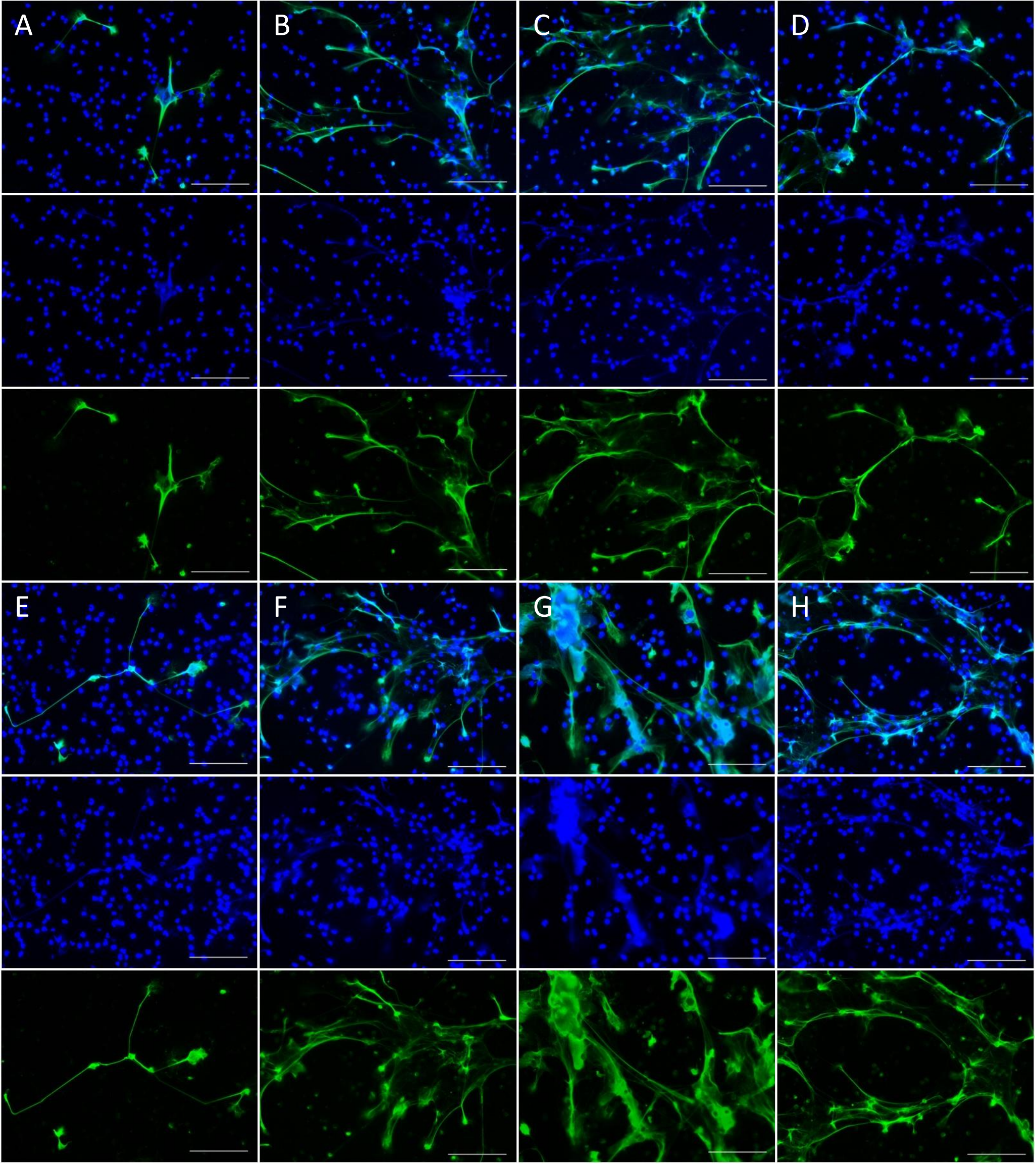


**Supplemental Figure 3. Single color for Figure 1 (NET dynamics in SIV infection)** NET identification: staining for lactoferrin (green); neutrophil nuclear staining: DAPI (blue).

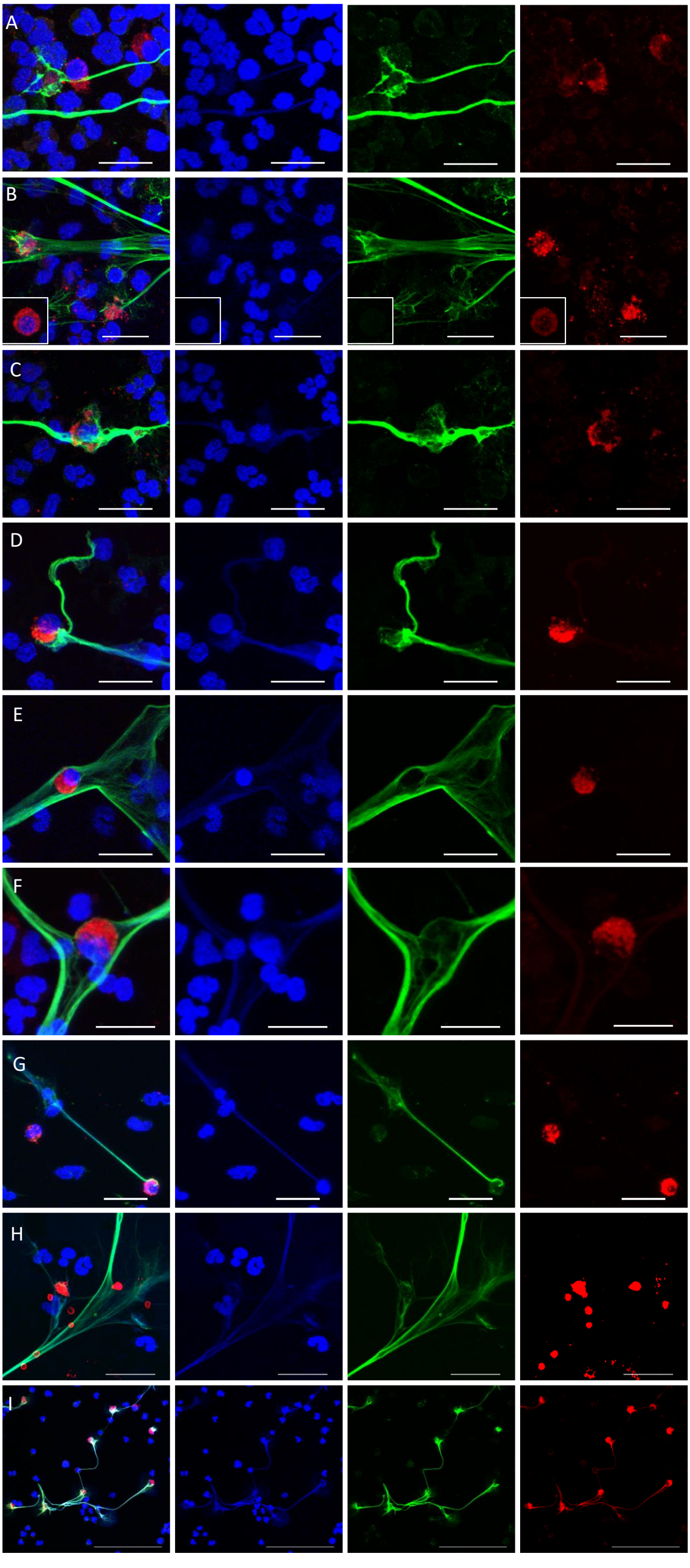


**Supplemental Figure 4. Single color for Figure 2 (Key collateral damage associated with excessive NET formation during SIV infection).** NET identification: staining for lactoferrin (green). CD4 (red) (A-C), CD8 (red) (D), CD20 (red) (E), CD163 (red) (F), SIV-infected cells (red) (G), platelets (red) (H), and TF (red) (I). Nuclear staining: DAPI (blue). Stimulated neutrophils (A-H); Unstimulated neutrophils (I).

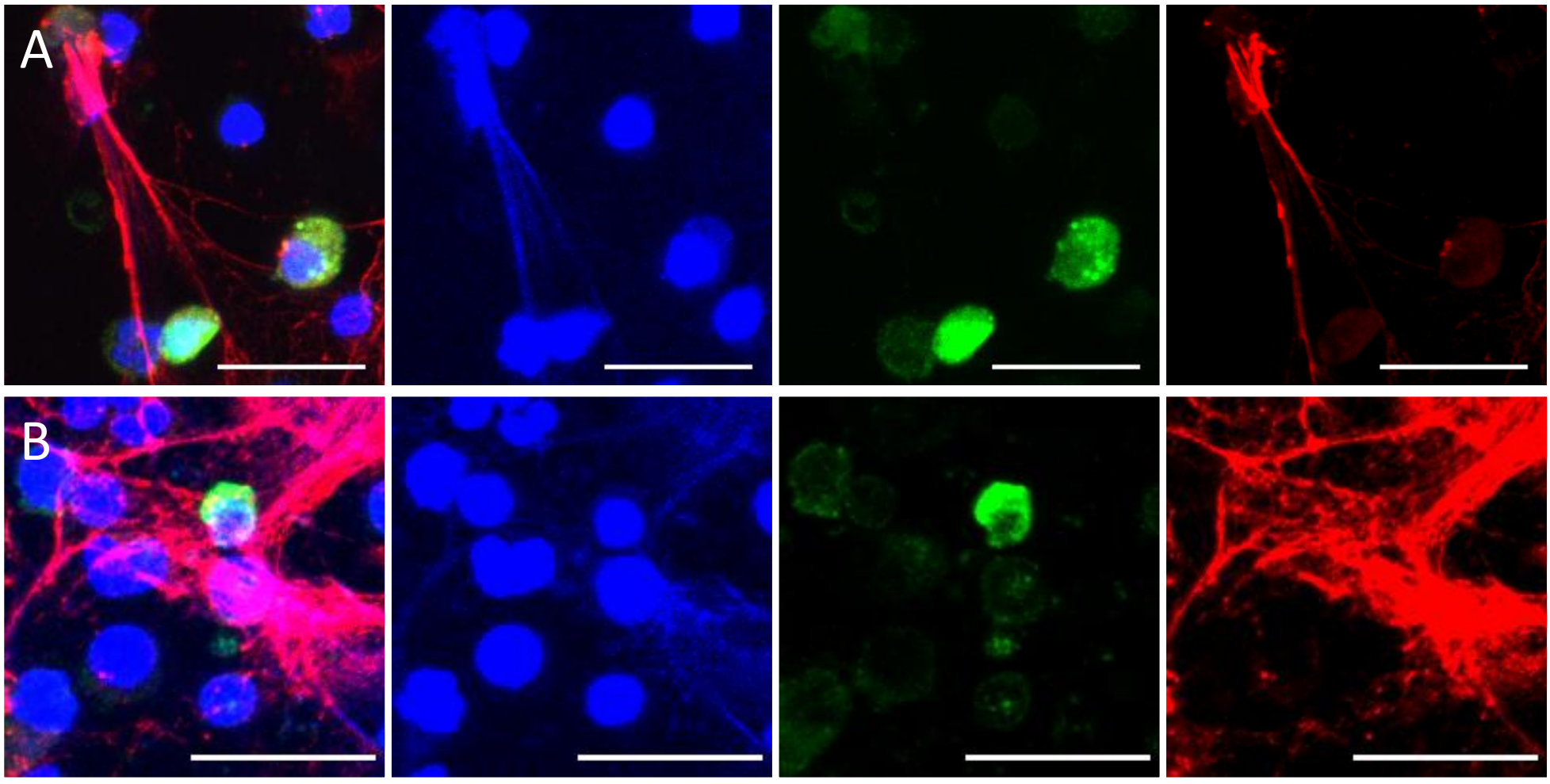


**Supplemental Figure 5. Single color for Figure 3 (Cell death in NETs).** Active caspase-3 (green), NET identification: staining for elastase (red); nuclear staining: DAPI (blue). Scale bar lengths: 20 µm.

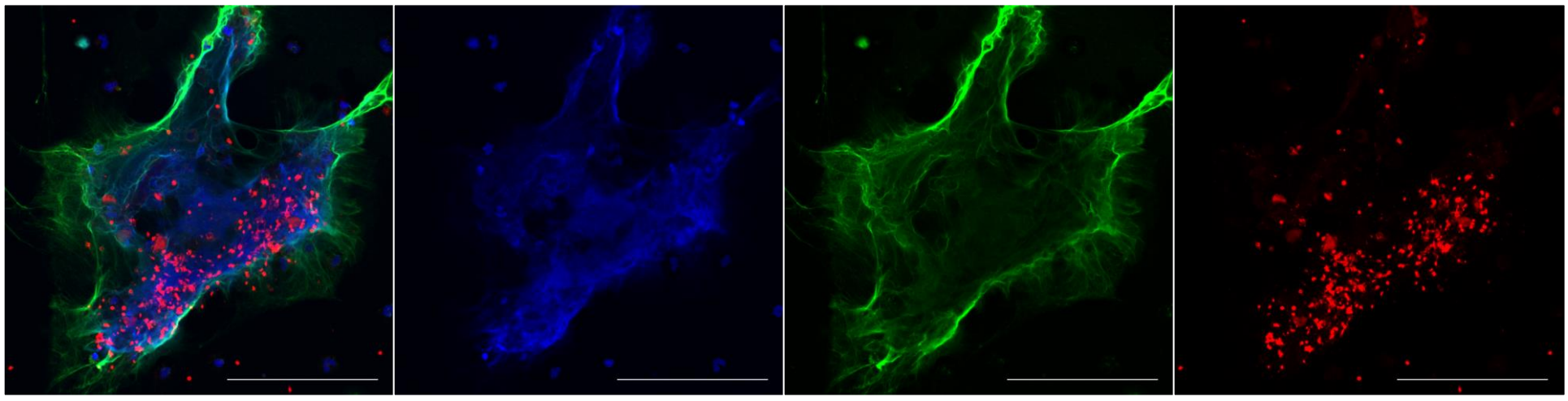

**Supplemental Figure 6. Platelet trapping and aggregation in NETs.** Large NETs, stained with lactoferrin (green), with numerous aggregated platelets (red). Nuclear staining: DAPI (blue). Scale bar lengths: 100 µm. Stimulated neutrophils are shown.

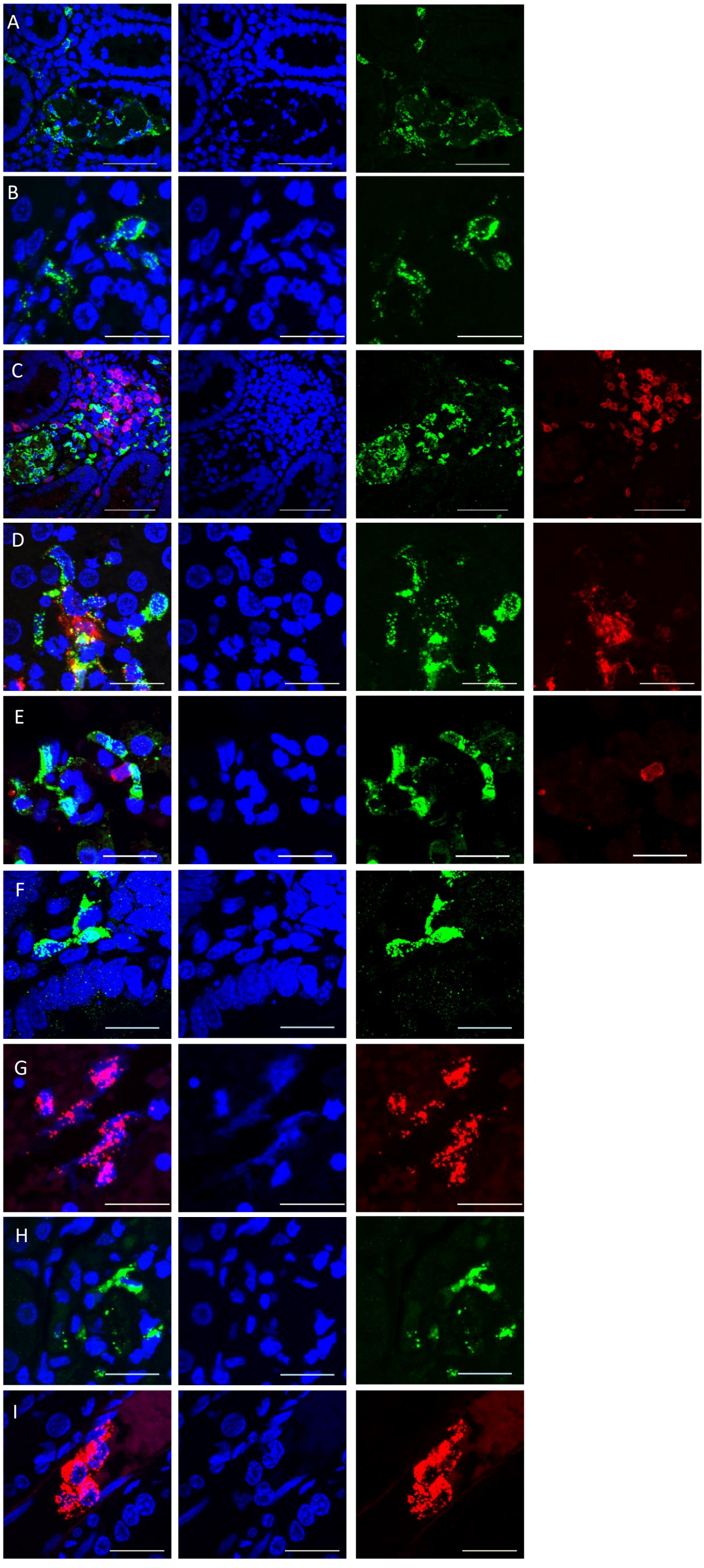


**Supplemental Figure 7. Single color for Figure 4 (Assessment of NETs in tissues).** NET identification: staining for MPO (green) (A-F and H) and NE (red) (G and I). $CD3^+$ T cells (red) (C and E); $CD68^+$ macrophages (red) (D). Nuclear staining: DAPI (blue). Scale bar lengths: 50 µm (A, C); 20 µm (B, and D-I).

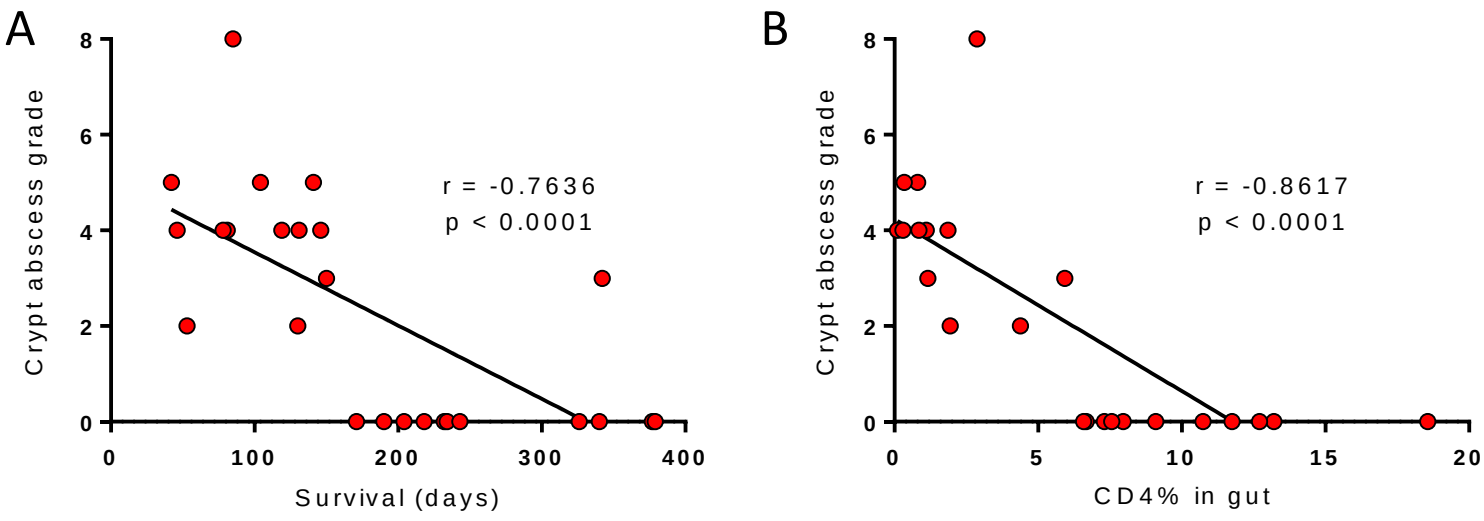


**Supplemental Figure 8. High NET frequency in the gut is indicative of poor prognosis.** The crypt abscess grade in the gut inversely correlated with survival (A), and with mucosal $CD4^+$ T cells (B). Spearman's rank correlation test; *r* and p values are shown as exact values. Significant correlation is illustrated as a solid line.

## METHODS

***Animals and infections.*** Thirty-seven pigtailed macaques (PTMs, *Macaca nemestrina*) aged 4 to 6 years old, and originating from the Washington National Primate Research Center, Seattle, WA, and Johns Hopkins University in Baltimore, MD, were included in this study. Ten PTMs were intravenously inoculated with plasma equivalent to 300 tissue culture infectious doses (TCID50) of SIVsab92018 and used to assess NET dynamics during SIV infection. The impact of ART on NET formation was evaluated in twelve additional SIVsab-infected PTMs receiving 10 months of coformulated ART (1) initiated at 50 days postinfection (dpi). These PTMs were virologically suppressed below the detection limit (30 vRNA copies/ml) at the time of the study. Ten PTMs were used as uninfected controls. Five additional uninfected PTMs were used for apoptosis studies. Tissues from 25 chronically SIV-infected PTMs from previous studies were used for histology.

***Sampling and sample processing.*** Blood was collected in sodium citrate anticoagulant (3.2 %) collection tubes. Samples were maintained at room temperature throughout the isolation procedure to prevent nonspecific neutrophil and platelet activation, and were processed within one hour from collection. To collect the platelet-rich plasma (PRP), samples were centrifuged at 150 *g* for 15 minutes, with the centrifuge allowed to slow without braking. The PRP layers were aspirated into fresh tubes and centrifuged for 5 minutes at 2,000 rotations per minute (863 *g*) to obtain platelet pellets; supernatants were removed to obtain platelet-poor plasma (PPP). The platelet pellets were washed once with platelet wash buffer (2) and resuspended in Tyrode's buffer (2)

and counted. Peripheral blood mononuclear cells (PBMCs) were separated from the remaining original tube contents (consisting of erythrocytes and leukocytes), by density gradient using Histopaque-1077 (Sigma-Aldrich, St. Louis, MO). Briefly, after centrifugation, the mononuclear cell layer was removed and the fraction containing the PMNs was collected and moved in a new tube where the erythrocytes were lysed with Ammonium-Chloride-Potassium (ACK) lysing buffer. This procedure results in ~95% purity of neutrophils as determined by the expression of $CD11b^{high}$ $CD14^{neg}$ markers by flow cytometry.

**Ex vivo NET identification/quantification.** One hundred thousand PMNs suspended in RPMI 1640, 1X (Corning, Corning, NY) containing 5% heat-inactivated newborn calf serum, 0.01% penicillin-streptomycin, 0.01% L-glutamine, and 0.01% HEPES buffer, were seeded on poly-D-lysine coated coverslips (Corning), placed in 24 well culture plates, and treated with 100 nM PMA (Cayman Chemical, Ann Arbor, MI), *Staphylococcus aureus* (Wood strain without protein A) BioParticles, Alexa Fluor 594 conjugated (Invitrogen, ThermoFisher Scientific, Waltham, MA), *Escherichia coli* (K-12 strain) BioParticles Alexa Fluor 594 conjugated (Invitrogen), or left unstimulated at 37°C for 2 hours. Cells were fixed with 4% PFA, blocked with 2% BSA in PBS, incubated with primary antibodies diluted in 2% BSA: rabbit anti-Histone H3 (1:100 dilution) (ab5103, Abcam, Cambridge, UK), rabbit anti-myeloperoxidase (1:800 dilution) (A0398, Agilent Technologies, Santa Clara, CA), rabbit anti-lactoferrin (1:1000 dilution) (L3262, Sigma-Aldrich), or mouse anti-neutrophil elastase (NE) (1:100 dilution) (clone NP57, Agilent Technologies) and then incubated with secondary antibodies donkey anti-rabbit Alexa Fluor® 488 conjugated (1:100 dilution) (ab150061, Abcam) or goat anti-mouse Alexa

Fluor 488 (1:150 dilution) (A21121, Invitrogen). Specimens were mounted in DAPI Fluoromount-G (SouthernBiotech, Birmingham, AL) on Superfrost Plus microscope slides (Fisherbrand, ThermoFisher Scientific) and visualized and imaged with Zeiss Imager M1 microscope and Axiovision software version 4.8.2.0 (Carl Zeiss AG, Oberkochen, Germany). Twenty images at 800x of slides stained with lactoferrin were used for quantification, which was performed using Fiji ImageJ software (3). For all images, positive signal was isolated *via* color threshold, and the percent area positive was measured and averaged.

**Picogreen NET quantification.** To quantify NET formation, we utilized the method of Fuchs et al. (4), with slight modifications. Briefly, $10^6$ purified PMNs in 200 µl of media (RPMI-1640 without phenol red red supplemented with 2% of inactivated serum from an uninfected PTM, L-glutamine, penicillin/streptomycin and 50mM Hepes) were either stimulated with 100 nM PMA (Cayman Chemical) or not stimulated, at 37°C with 5% $CO_2$ in an incubator with rotation at 50 rpm for 90 minutes. Then, nuclease digestion was performed with 0.1 U of micrococcal nuclease from *S. aureus* (Sigma-Aldrich) for 10 minutes at 37°C. Nuclease activity was stopped with 0.005 M EDTA (ThermoFisher Scientific), and cellular debris were removed by centrifugation. Culture supernatants were collected and stored at 4°C overnight. DNA content was measured with the Quant-iT™ Picogreen dsDNA Assay Kit (Invitrogen), according to manufacturer's instructions.

**NET quantification in plasma.** A sandwich ELISA developed by Mark Looney's group was used to detect soluble NET components, namely NE-DNA complexes in the plasma collected from the SIV-infected PTMs. NET ELISA was performed as described (5), using antibodies against NE (Agilent) and an anti-DNA-HRP conjugate (Cell Death

Detection ELISA Kit, Roche). We performed this ELISA on the same groups of PTMs for which the above ex vivo quantifications were performed.

**Immune cell trapping in the NETs.** One hundred thousand PMNs were seeded along with $1X10^5$ PBMCs or $1X10^5$ platelets on poly-D-lysine coated coverslips (Corning), and incubated with 100 nM PMA (Cayman Chemical) at 37°C for 2 hours. The cell handling and NET IHC were performed as described above. NET identification was done with the rabbit anti-lactoferrin. Cells were then incubated with the following monoclonal antibodies: mouse anti-CD4 (1:25 dilution) (clone 4B12, Agilent Technologies), mouse anti-CD8 (1:50 dilution) (NCL-L-CD8-4B11, Leica Biosystems, Wetzler, Germany), mouse anti-CD20 (1:50 dilution) (clone L26, Agilent Technologies), mouse anti-CD163 (1:20 dilution) (clone GHI/61, Biolegend, San Diego, CA), or a mouse anti-CD42a (1:20 dilution) (clone ALMA.16, Biolegend), and then with the goat anti-mouse secondary antibody (1:100 dilution) conjugated with Alexa Fluor 568 (A21124, Invitrogen). Specimens were mounted in DAPI Fluoromount-G (Southern Biotech) on Superfrost Plus microscope slides (Fisherbrand) and visualized with an Olympus Fluoview FV 1000 confocal microscope. Images were processed with NIS-Elements AR 5.0 (Nikon Instruments, Tokyo, Japan). Number of cells caught in NETs and cells present out of NETs for each subset were manually counted in 20 fields at 800x magnification.

**Tissue Factor expression in PMNs and NETs.** One hundred thousand PMNs were incubated for 2 hours with or without PMA stimulation as described above, and then stained with rabbit anti-lactoferrin (Sigma-Aldrich) followed by an incubation with the secondary antibody, donkey anti-rabbit conjugated with Alexa Fluor® 488 (Abcam) and

then stained with mouse anti-CD142 (clone HTF-1, Beckton Dickinson, NJ) followed by goat anti-mouse secondary antibody conjugated with Alexa Fluor 568 (Invitrogen). Specimens were mounted in DAPI Fluoromount-G (Southern Biotech) on Superfrost Plus microscope slides (Fisherbrand) and visualized with an Olympus Fluoview FV 1000 confocal microscope. Images were processed with NIS-Elements AR 5.0 (Nikon Instruments, Tokyo, Japan).

**Apoptosis assessment**

**a) Indirect *apoptosis* assessment through flow cytometry*.*** One million PMNs were incubated alone or with $1X10^6$ PBMCs suspended in 300 µl of media and were either stimulated or not stimulated with 100 nM PMA for 2 or 4 hours, following which nuclease digestion was performed with 0.1 U of micrococcal nuclease from *S. aureus* for 10 minutes at 37°C. Nuclease activity was stopped with 0.005 M EDTA, and cells were washed with Annexin V Binding Buffer (Beckton Dickinson). Flow cytometry staining was performed with Viability blue dye (Invitrogen), CD3 (clone SP34-2), CD4 (clone L200), CD8 (clone RPA-T8), Annexin V (clone 556419), all from Beckton Dickinson, and acquired on an LSR II (Beckton Dickinson). Data was analyzed with FlowJo v10 (FlowJo LLC, Ashland, OR).

**b) Direct apoptosis assessments through immunofluorescence.** One hundred thousand PMNs were incubated for 2 hours along with $1X10^5$ PBMCs as described above. They were then stained with rabbit anti-active caspase-3 (1:50 dilution) (ab2302, Abcam) followed by a donkey anti-rabbit secondary antibody conjugated with Alexa Fluor® 488 (ab2302 Abcam) (1:100 dilution), and then with a mouse anti-NE (1:100 dilution) followed

by a goat anti-mouse secondary antibody conjugated with Alexa Fluor 568 (Invitrogen) (1:150 dilution). Apoptotic cells caught in NETs and apoptotic cells present out of NETs were manually counted in 30 fields at 800x magnification.

**NET identification in tissues.** Immunofluorescence staining was performed on formalin-fixed, paraffin-embedded tissue samples. Sections four μm thick were deparaffinized and rehydrated. For the MPO staining, the antigen retrieval was performed by microwaving in Vector Unmasking Solution (Vector Laboratories Burlingame, CA). Sections were incubated with the anti-MPO primary antibody (1:800 dilution) (A0398, Agilent Technologies) followed by and incubation with donkey anti-rabbit conjugated with Alexa Fluor® 488 (Abcam) (1:100 dilution) and then, if double staining was done, this step was followed by an incubation with either anti-CD3 (1:25 dilution) (A0452, Agilent Technologies) or anti-CD68 (1:25 dilution) (clone KP1, Agilent Technologies), followed by a goat anti-mouse secondary antibody conjugated with (1:150 dilution) Alexa Fluor 568 (Invitrogen). A similar protocol was used for staining for neutrophil elastase (NE), except that antigen retrieval was done by incubating the tissues at 50°C for 90 minutes (6), and followed by an incubation with the anti-NE primary antibody (1:50 dilution) (Agilent Technologies) and then with a goat anti-mouse secondary antibody conjugated with Alexa Fluor 568 (1:150 dilution). The tissues were then incubated with DAPI (1:5000 dilution) (Millipore Sigma, Burlington, MA) for nuclear staining, followed by Trueblack lipofuscin autofluorescence quencher (1:20 dilution in 70% ethanol) (Biotium Inc, Hayward, CA), to suppress autofluorescence. Slides were finally cover-slipped using fluorescent mounting media (Agilent) and coverslips (Thermo Fisher Scientific).

***Virion capture visualization through RNAScope.*** One hundred thousand PMNs and $1X10^5$ PBMCs isolated from chronically SIVsab-infected PTMs with high viral loads were seeded in CC2 coated Chamber Slides (Lab-Tek, ThermoFisher), in media with 100 nM PMA and incubated at 37°C for 2 hours. Cells were fixed with 10% neutral buffered formalin for 30 minutes and then washed with PBS. The slides were treated with Protease III (ACD Biotech, Toronto, Canada) for 10 minutes, and then washed with PBS. RNAscope was then performed according to manufacturer specifications using Probe-V-SIVagm and Amp 4 Alt-B (ACD Biotech), as described (7), and imaged on Olympus Fluoview 1000 Confocal Microscope. Images were processed with NIS-Elements AR 5.0 (Nikon). Following RNAscope, immunofluorescence staining was performed on the slides for lactoferrin, as described above, and imaged on an Olympus Fluoview 1000 Confocal Microscope.

**Crypt abscess grading.** Hematoxylin and eosin stain was performed on jejunums obtained from necropsy of PTMs infected with SIVsab, and graded for crypt abscesses on a scale from 0 to 10.

***Statistics.*** All graphing and statistical analyses were carried out using Prism 7 (GraphPad Software, San Diego, CA). Data was expressed as means ± standard errors of the means (SEM). To compare the differences in NET production between timepoints, two-tailed Mann-Whitney U test with Bonferroni correction for multiple comparisons was used. To compare differences in levels of apoptosis between PBMC only and PBMC with PMN tubes, two-tailed Mann-Whitney *U* test was used; $p<0.05$ was considered significant. To compare differences in cell trapping, and to compare number of apoptotic cells caught in NETs to those not caught in NETs, two-tailed Wilcoxon test was used;

$p<0.05$ was considered significant. To compare the number of apoptotic cells caught in NETs to those not caught in the NETs, one-tailed Wilcoxon test was used; $p<0.05$ was considered significant. Correlations between crypt abscess grading and survival and between crypt abscess grading and gut CD4% were performed using Spearman's rank correlation.

## References


1. Del Prete GQ, Smedley J, Macallister R, Jones GS, Li B, Hattersley J, et al. Short communication: Comparative evaluation of coformulated injectable combination antiretroviral therapy regimens in simian immunodeficiency virus-infected rhesus macaques. *AIDS Research and Human Retroviruses.* 2016;32(2):163-8.
2. Green SA, Smith M, Hasley RB, Stephany D, Harned A, Nagashima K, et al. Activated platelet–T-cell conjugates in peripheral blood of patients with HIV infection: coupling coagulation/inflammation and T cells. *AIDS (London, England).* 2015;29(11):1297-308.
3. Schneider CA, Rasband WS, and Eliceiri KW. NIH image to imageJ: 25 years of image analysis. *Nature methods.* 2012;9(7):671-5.
4. Fuchs TA, Abed U, Goosmann C, Hurwitz R, Schulze I, Wahn V, et al. Novel cell death program leads to neutrophil extracellular traps. *The Journal of cell biology.* 2007;176(2):231-41.
5. Lefrançais E, Mallavia B, Zhuo H, Calfee CS, and Looney MR. Maladaptive role of neutrophil extracellular traps in pathogen-induced lung injury. *JCI Insight.* 2018;3(3).
6. Brinkmann V, Abu Abed U, Goosmann C, and Zychlinsky A. Immunodetection of NETs in paraffin-embedded tissue. *Frontiers in immunology.* 2016;7:513.
7. Wang F, Flanagan J, Su N, Wang LC, Bui S, Nielson A, et al. RNAscope: a novel in situ RNA analysis platform for formalin-fixed, paraffin-embedded tissues. *The Journal of molecular diagnostics : JMD.* 2012;14(1):22-9.

**Supplemental Table 1. Nominal p-value results of Mann-Whitney tests in figures 1I , 1J, and 1K.**

| | Immunofluorescence NET quantification | | Picogreen NET quantification | | NET ELISA |
|---|---|---|---|---|---|
| | Unstimulated | Stimulated | Unstimulated | Stimulated | |
| **$SIV^{neg}$ *vs* Acute** | 0.0000108 | 0.0000108 | 0.01854 | 0.000206 | 0.03546 |
| **$SIV^{neg}$ *vs* Chr.** | 0.000103 | 0.000103 | 0.003085 | 0.00195 | 0.00463 |
| **$SIV^{neg}$ *vs* Chr. ART** | 0.00564 | 0.003436 | 0.01338 | 0.1072 | 0.531 |
| **Chr. *vs* Chr. ART** | 0.02211 | 0.01298 | 0.03108 | 0.00524 | 0.163 |

In the figure, significance is defined after applying Bonferroni correction because of double comparison between $SIV^{neg}$ *vs* acute and $SIV^{neg}$ *vs* Chr. Note that the comparisons between $SIV^{neg}$ *vs* Chr ART, and Chr *vs* Chr ART used independent groups of animals. $SIV^{neg}$-unifected pigtailed macaques; Acute-acute SIV infection; Chr-chronic SIV infection; Chr ART-chronic SIV infection treated with antiretrovirals

**Supplemental Table 2: Survival, CD4$^+$ T cell counts and crypt abscess grading in SIV-infected pigtailed macaques**

| Animal Number | Survival (Days) | Gut CD4 (%) | Crypt abscess grading |
|---|---|---|---|
| PTM1 | 42 | 0.336 | 5 |
| PTM2 | 46 | 1.81 | 4 |
| PTM3 | 53 | 1.94 | 2 |
| PTM4 | 78 | 0.85 | 4 |
| PTM5 | 81 | 1.86 | 4 |
| PTM6 | 85 | 2.87 | 8 |
| PTM7 | 104 | 0.36 | 5 |
| PTM8 | 119 | 1.1 | 4 |
| PTM9 | 130 | 4.38 | 2 |
| PTM10 | 131 | 0.11 | 4 |
| PTM11 | 141 | 0.8 | 5 |
| PTM12 | 146 | 0.3 | 4 |
| PTM13 | 150 | 1.16 | 3 |
| PTM14 | 171 | 12.71 | 0 |
| PTM15 | 190 | 7.96 | 0 |
| PTM16 | 204 | 10.74 | 0 |
| PTM17 | 218 | 9.1 | 0 |
| PTM18 | 232 | 13.2 | 0 |
| PTM19 | 234 | 7.3 | 0 |
| PTM20 | 243 | 6.67 | 0 |
| PTM21 | 326 | 11.75 | 0 |
| PTM22 | 340 | 6.58 | 0 |
| PTM23 | 342 | 5.93 | 3 |
| PTM24 | 377 | 18.56 | 0 |
| PTM25 | 379 | 7.56 | 0 |